ELSEVIER

Earth and Planetary Science Letters 206 (2003) 541–553

EPSL

www.elsevier.com/locate/epsl

Magnetic state of 10–40 Ma old ocean basalts and its implications for natural remanent magnetization

Jürgen Matzka *, David Krása, Thomas Kunzmann, Axel Schult, Nikolai Petersen

Department for Earth and Environmental Sciences, Ludwig-Maximilians-Universität München, Theresienstr. 41, 80333 Munich, Germany

Received 5 August 2002; received in revised form 21 November 2002; accepted 21 November 2002

Abstract

The natural remanent magnetization (NRM) of ocean basalts, giving rise to the pattern of marine magnetic anomalies, is known to be of comparatively low intensity for about 20 Ma old oceanic crust. The aim of this study is to detect possible peculiarities in the rock magnetic properties of ocean basalts of this age, and to establish a link between magnetomineralogy, rock magnetic parameters, and the low NRM intensity. Ocean basalts covering ages from 0.7 to 135 Ma were selected for rock magnetic experiments and their room temperature hysteresis parameters, Curie temperature and temperature dependence of saturation magnetization $M_S(T)$ was determined and complemented by reflected light microscopy. The majority of samples is magnetically dominated by titanomagnetite and titanomaghemite with increasing oxidation state with age. For these, a strong dependence of hysteresis parameters on the age of the samples is found. The samples have a minimum in saturation magnetization and a maximum in magnetic stability in the age interval ranging from approximately 10 to 40 Ma, coinciding with the age interval of low NRM intensity. The observed change in saturation magnetization is in the same order as that for the NRM intensity. A further peculiarity of the titanomaghemites from this age interval is the shape of their $M_S(T)$ curves, which display a maximum above room temperature (Néel P-type) and, sometimes, a self-reversal of magnetization below room temperature (Néel N-type). These special rock magnetic properties can be explained by titanomagnetite low-temperature oxidation and highly oxidized titanomaghemites in the age interval 10–40 Ma. A corresponding measurement of the NRM at elevated temperature allows to identify a maximum in NRM intensity above room temperature for the samples in that age interval. This provides evidence that the NRM is equally carried by titanomaghemites and that the low NRM intensities for about 20 Ma old ocean basalts are caused consequently by the low saturation magnetization of these titanomaghemites.
© 2002 Elsevier Science B.V. All rights reserved.

Keywords: ocean basalt; rock magnetism; titanomaghemite; low-temperature oxidation; maghemitization

1. Introduction

The most important carriers of natural remanent magnetization (NRM) in ocean basalts are titanomagnetites of composition similar to TM60

* Corresponding author. Tel.: +49-89-2180-4143; Fax: +49-89-2180-4205.
E-mail address: matzka@geophysik.uni-muenchen.de (J. Matzka).

0012-821X/02/$ – see front matter © 2002 Elsevier Science B.V. All rights reserved.
doi:10.1016/S0012-821X(02)01094-4

($Fe_{3-x}Ti_xO_4$ with $x = 0.6$) and their low-temperature oxidation products, the titanomaghemites [1–4]. The degree of this low-temperature oxidation or maghemitization is given by the parameter z, which is defined as the ratio of oxidized Fe^{2+} to original Fe^{2+} [5] and ranges from 0 (unoxidized) to 1 (fully oxidized). The oxidation proceeds slowly [3,4,6], typically on a time scale of several million years (Ma). The direction of NRM acquired by the titanomagnetites at mid-ocean ridges is preserved during the oxidation process [7], leading to the oceanic magnetic anomalies first explained by Vine and Matthews [8].

However, the mean NRM intensity of ocean basalts, when averaged over an appropriate age interval, shows a peculiar variation with age. First, the NRM decreases with age (or distance to the ridge axis), having then a minimum for approximately 20 Ma old ocean basalts. The mean NRM intensities in the age interval 10–30 Ma are $\approx 70\%$ lower than for 0–5 Ma old ocean basalts. For older ocean basalts, beyond that age interval, the NRM increases again. This phenomenon is known both from directly measured NRM intensities of ocean basalts recovered by the Deep Sea Drilling Project (DSDP) and Ocean Drilling Program (ODP) [9–11], as well as from the inversion of magnetic anomalies [12–14].

Several mechanisms have been suggested to explain the minimum in NRM intensity for approximately 20 Ma old ocean basalts. One mechanism is the decrease of NRM intensity in the first 20 Ma by maghemitization [2,9,10], whereas the NRM increase for older crust was thought to be due to a higher content of magnetic minerals in these rocks [10], or also to maghemitization [9]. A different approach is to explain the change in NRM intensity by a delayed NRM acquisition leading to a inverse relationship of NRM intensity and reversal rate [15,16], or by long-term changes in the strength of the Earth's magnetic field [17].

If the NRM intensities are in fact controlled by maghemitization, this should also have a strong effect on the rock magnetic properties. In this study, the magnetomineralogy of a great number of ocean basalts covering all oceans is studied and the dependence of rock magnetic properties on age and on titanomaghemite oxidation state is determined. Additionally, the measurement of NRM at elevated temperature is used to characterize some of the samples.

2. Samples and techniques

A total of 93 samples collected both by the Ocean Drilling Program (ODP) and the Deep Sea Drilling Program (DSDP) from 51 different drilling sites were studied. The samples were selected on the basis of only one criterion, i.e. their description as ocean floor basalt in the corresponding Initial or Scientific Report published by ODP/DSDP. We tried a random sampling strategy to average out small scale variations like the distance to the margin of a pillow, which can significantly influence its magnetic properties [18]. No samples were taken from ODP site 504B, which is typified by basalts containing chromium spinels, and site 597C, which have high-temperature (deuterically) oxidized titanomagnetites. Although grain size and permeability to seawater can play an important role for titanomagnetite/titanomaghemite oxidation state and magnetic properties [11], a further lithological distinction sensitive to these parameters, e.g. between flows and pillow lavas, was not attempted for two reasons. Firstly, previous studies that reveal age trends for magnetic properties of ocean basalts included both pillow lavas and flows [9,10]. Secondly, the inversion of oceanic magnetic anomalies leads to similar results [13,14] for both the Atlantic Ocean with slow spreading rate where pillow lavas dominate and the Pacific Ocean with fast spreading rates where flows dominate [19]. The samples shown here are from the Atlantic (26 sites), Pacific (23 sites), Indian Ocean (one site) and the Mediterranean Sea (one site). The ages of the samples for each site were taken from either the Initial Reports of the ODP/DSDP or, when applicable, from a more recent compilation [17]. The ages range from 0.7 to 135 Ma.

For the magnetic measurements, small cores of 5 mm diameter and a few mm length were drilled from the inch-sized cylinders provided by ODP/DSDP. Hysteresis loops at room temperature

were measured with a variable field translation balance (VFTB, maximum magnetic field H = 0.63 T). Prior to the calculation of hysteresis parameters, the paramagnetic content was estimated by a linear fit between 0.5 and 0.63 T and subtracted from the hysteresis loops. Thermomagnetic curves were obtained with the VFTB by measuring the induced magnetization from room temperature to 600°C in air at saturating fields as determined from the hysteresis loops (a field of 0.4 T was used for samples which could not be magnetically saturated). Curie temperatures T_C were determined with the tangent method [20].

Magnetic hysteresis loops on a subset of 11 samples were measured at and below room temperature with a Princeton Measurements Vibrating Sample Magnetometer (μ-VSM, maximum magnetic field H = 1.7 T, paramagnetic content determined between 1.4 and 1.7 T) at the Institute for Rock Magnetism (IRM), University of Minnesota. On a subset of five samples, magnetic hysteresis loops at and below room temperature were measured with a Magnetic Properties Measurement System (MPMS, maximum magnetic field 5 T, paramagnetic content determined between 2 and 5 T) at the IRM. The MPMS was additionally used for measuring zero-field-cooling curves of a saturation isothermal remanent magnetization (SIRM) between 27 and −263°C (300 and 10 K).

On a further subset of six samples, the NRM was measured during heating from room temperature to 600°C. For this purpose a fluxgate spinner magnetometer with an integrated oven was built. It measures the component of the NRM intensity perpendicular to the spinning axis. Details of this instrument, which is referred to as 'Hotspin' magnetometer, can be found in [21].

Lattice constants a_0 were determined on magnetic extracts from three samples with a Guinier-type camera. The extracts were mixed with SiO_2 powder as a standard and measured with Co $K_{\alpha 1}$ radiation using an imaging plate in asymmetric back-reflection configuration. The lattice constant of the titanomagnetite/titanomaghemite was determined from reflection peaks in the interval $37° < \theta < 89°$. Composition parameters x and z were determined from the T_C and a_0 contour diagrams of Readman and O'Reilly [22], a possible influence of cations other than Fe and Ti was neglected.

Polished sections were made from 30 randomly selected samples and studied microscopically with a Leitz Ortholux Pol polarization microscope.

3. Results

3.1. Magnetomineralogy

Titanomagnetites or titanomaghemites were identified in all samples studied by light microscopy as the dominating magnetic mineral. Additionally, most samples contain significant amounts of hemoilmenites, which can be distinguished from the titanomagnetites and titanomaghemites by their strong optical anisotropy [23]. Some samples also contain a minor amount of iron sulfides. From previous studies [4] it can be expected that the hemoilmenites have Curie temperatures below room temperature and also that there is no significant contribution from iron sulfides to the magnetization of ocean basalts.

On the basis of thermomagnetic analyses, the samples can be divided into several groups according to their magnetomineralogy. As will be shown below, the majority of samples contain titanomaghemite, rather than titanomagnetite.

A total of 12 samples will not be further discussed here. These are five samples with one magnetic phase with T_C between 565 and 575°C (exsolved titanomagnetite due to deuteric oxidation) and seven samples having two Curie temperatures with the higher T_C corresponding to a low-temperature oxidized TM60 and the lower T_C being below 120°C. The latter samples probably contain primary hemoilmenites with abnormally low Ti content as a second magnetic mineral phase, or (impurity cation-rich) titanomagnetites.

In Fig. 1a, the Curie temperatures of the remaining 81 samples are plotted versus the age of the samples. As will be discussed later, 18 of the samples older than 40 Ma display two Curie temperatures of which only the lower T_C is shown in Fig. 1a. These samples with two magnetic phases will be referred to as the 2-T_C-group. The ocean

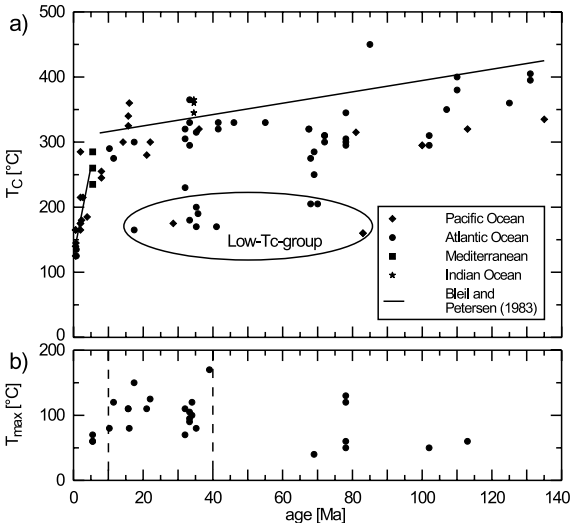

Fig. 1. Curie temperature T_C plotted against age of the samples (a). Most samples follow the trend of T_C with age described by Bleil and Petersen [9]. Some samples older than 15 Ma not following this trend are marked (Low-T_C-group). For samples with a maximum in the thermomagnetic curve the temperature of maximum magnetization T_{max} is plotted in panel b.

from which the samples originate is indicated in order to demonstrate the good coverage of age for samples both from the Atlantic and Pacific Ocean.

The Curie temperatures follow the age trend observed by Bleil and Petersen [9], which is characterized by a steep increase of T_C from $\approx$125°C to $\approx$300°C in the first 10 Ma and a much less pronounced increase with age for older samples. This behavior reflects the low-temperature oxidation of the titanomagnetites in ocean basalts with age.

A few of the samples with one magnetic phase do not follow that general trend, but have a Curie temperature which is lower than that typical for their age. This group is defined as to contain samples older than 15 Ma with $T_C \leq 205$°C. These are 11 samples and will be referred to as Low-T_C-group (see Fig. 1a).

Remaining are 52 samples with one magnetic phase which has a Curie temperature according to the trend for titanomagnetite low-temperature oxidation in ocean basalts. They are referred to as Tmgh-group. The criteria to distinguish between samples of the Tmgh-group and 2-T_C-group are further elaborated below.

The thermomagnetic curves of some samples with $T_C \geq 230$°C displayed a maximum of the induced magnetization above room temperature. The temperature at which this maximum occurs is denoted T_{max} (T_{max} was determined graphically from the thermomagnetic curves with an accuracy of 5°C) and plotted versus age in Fig. 1b. This behavior is typical for the 10–40 Ma old samples of the Tmgh-group, where 18 of 20 samples show a maximum above room temperature and where T_{max} has the highest values. It is scarcely found for younger ocean basalts (three of 20 Tmgh-group samples) and only for seven (six samples of the Tmgh-group and one sample of the 2-T_C-group) of the 30 samples older than 40 Ma. Hence, not only the Curie temperature but also the shape of the thermomagnetic curves is dependent on age and indicates a peculiar magnetic behavior in the age interval from $\approx$10 Ma to $\approx$40 Ma (marked in Fig. 1b).

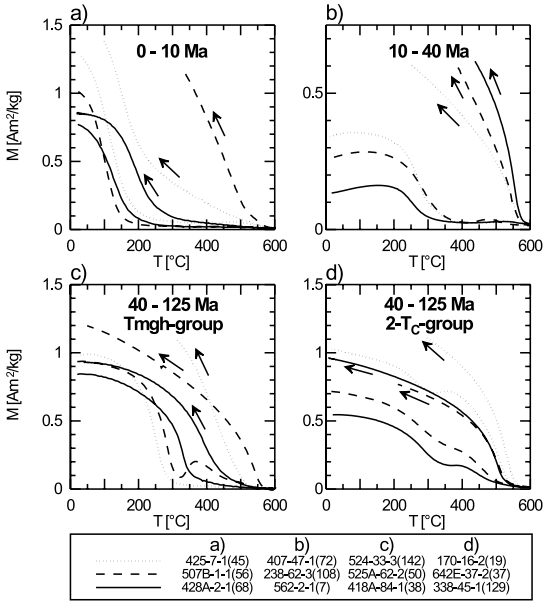

Fig. 2. Selected thermomagnetic curves (induced magnetization at saturating fields, or maximum field of 0.4 T) of samples from the Tmgh-group (a–c) and 2-T_C-group (d). To account for the low magnetization of the 10–40 Ma old Tmgh-group samples, the magnetization axes in panel b are different from those in a, c and d. Cooling curves are indicated by arrows.

Selected thermomagnetic curves are shown in Fig. 2 in order to demonstrate this dependence on age for the Tmgh-group and the difference between the Tmgh-group and the 2-T_C-group. The induced magnetization of the youngest samples (<10 Ma, Fig. 2a) typically decreases between room temperature and their Curie temperatures. The maximum of the induced magnetization above room temperature for the 10–40 Ma old samples of the Tmgh-group is shown in Fig. 2b. This maximum is absent or shifted to lower temperatures for samples older than 40 Ma of the Tmgh-group (Fig. 2c). Samples assigned to the Tmgh-group are controlled by a titanomaghemite phase (although contributions in the order of a few percent to the induced magnetization from a second magnetic phase with higher Curie temperatures cannot be excluded). It can already be seen in Fig. 2 that the 10–40 Ma old samples of the Tmgh-group are not only characterized by a maximum in the induced magnetization above room temperature, but also by lower magnetizations at room temperature compared to the other samples. The first stage of titanomaghemite inversion can be observed in some of the heating curves by a rise of magnetization above $\approx$300°C (Fig. 2b,c), the final inversion product has Curie temperatures of $\approx$550°C (cooling curves) [24].

The thermomagnetic curves of the samples assigned to the 2-T_C-group (Fig. 2d) show significant contributions from two magnetic phases. The lower Curie temperature is typical for titanomaghemite and it is possible that the higher Curie temperature belongs to the first-stage inversion product of the titanomaghemite [24]. This interpretation is supported by the observed increase in magnetization above 300°C in the thermomagnetic curves for some of the samples. However, it cannot be excluded that the samples of the 2-T_C-group already contained the second magnetic phase before heating. It can therefore be expected that the Tmgh-group contains the samples most suitable to study the general effect of maghemitization on the magnetic properties of ocean basalts.

The temperature dependence of the saturation magnetization $M_S(T)$ (full line in Fig. 3) for 11 samples of the Tmgh-group was determined from hysteresis loops with a μ-VSM (maximum field of 1.7 T) measured every 15°C between −258°C (15 K) and 177°C (450 K). The three plots in the uppermost row of Fig. 3 represent samples of the Tmgh-group with ages between 0 and 10 Ma. Their $M_S(T)$ curves are characterized by a local maximum in M_S just below room temperature. The five plots in the second and third row of Fig. 4 show 10–40 Ma old samples of the Tmgh-group. Their $M_S(T)$ curves display a local maximum in M_S above room temperature. In the lowermost row, plots of Tmgh-group samples older than 40 Ma are shown. They again have a local maximum in M_S just below room temperature. The local maximum in the $M_S(T)$ curves of all samples can be explained by the titanomaghemite's ferrimagnetic behavior of P-, L- or N-type according to the definition by Néel [25].

Another common feature of the $M_S(T)$ curves for all samples in Fig. 3 is an additional increase of M_S towards lower temperatures, from $\approx$−100°C downwards. This most likely represents additional contributions to the magnetization by primary hemoilmenites, which were observed by optical microscopy. Furthermore, the composition of primary hemoilmenites coexisting with primary TM60 in ocean basalts is expected to be close to $Fe_{1.1}Ti_{0.9}O_3$ [26,27], which gives a Curie temperature ($T_C \approx -150$°C [28]) that is in good agreement with the observed increase of M_S.

The local maximum in M_S above room temperature for the 10–40 Ma old samples of the Tmgh-group can also be deduced from high-field hysteresis loop measurements (maximum field 5 T) with the MPMS at temperature intervals of 30°C between −93°C and 27°C (triangles in second and third row of Fig. 3), which closely follow the $M_S(T)$ curves measured with the μ-VSM. The reason for measuring these samples additionally with the MPMS is their high magnetic stability necessitating high magnetic fields to saturate the samples, as will be discussed later. Zero-field-cooling curves between 27 and −263°C of the SIRM imparted at 27°C in a field of 2.5 T were also measured for these samples (dotted line with arrow in Fig. 3). For three samples (572D-34-1(99) with $T_C = 360$°C, $a_0 = 8.372$ Å, $x = 0.53$, $z = 0.91$; 238-61-4(6) with $T_C = 365$°C, $a_0 = 8.379$ Å,

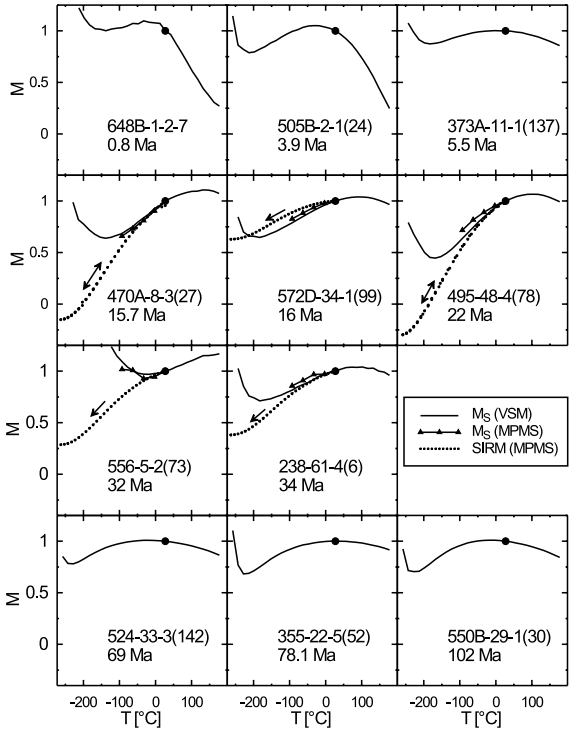

Fig. 3. Temperature dependence of the saturation magnetization $M_S(T)$ measured with the μ-VSM (full line) for Tmgh-group samples. The upper row shows samples younger than 10 Ma, the second and third row samples between 10 and 40 Ma, and the last row samples older 40 Ma. For the 10–40 Ma old samples additional $M_S(T)$ curves (triangles) and zero-field-cooling curves (dotted line) of a SIRM were measured with the MPMS (see text).

$x = 0.51$, $z = 0.88$ and 556-5-2(73)), the zero-field cooling showed a monotonous decrease of the SIRM with decreasing temperature. This indicates a ferrimagnetic behavior of Néel P-type for the titanomaghemites.

For the two samples 470A-8-3(27) and 495-48-4(78) (with $T_C = 300$°C, $a_0 = 8.398$ Å, $x = 0.57$, $z = 0.88$) zero-field cooling leads to a self-reversal of the SIRM at ≈ -180°C. At that temperature the SIRM decreases to zero and increases for lower temperatures again in the opposite direction (indicated by negative values in Fig. 3). For these two samples, the warming of the SIRM was measured subsequently to the cooling (double-headed arrows). As the cooling and warming curves are reversible, the temperature dependence of the SIRM can be attributed to the temperature dependence of the saturation magnetization. Both samples contain therefore titanomaghemite of Néel N-type. Note that the Néel N-type behavior also causes an increase in $M_S(T)$ for $T < -180$°C, additionally to that caused by primary hemoilmenite.

3.2. Age dependence of hysteresis parameters

Hysteresis loops for all samples of the Tmgh-group, 2-T_C-group, and Low-T_C-group were measured with the VFTB at room temperature in a maximum field of 0.6 T, which was not sufficient to saturate the magnetically most stable samples. The hysteresis parameters saturation magnetization M_S, coercive force H_C, and the ratio of saturation remanence to saturation magnetization M_{RS}/M_S are shown in Fig. 4. Despite the scatter of the data, especially for the samples older than 40 Ma, the samples of the Tmgh-group show significantly decreased values for M_S in the age interval from 10 to 40 Ma (marked in Fig. 4), which are accompanied by a high magnetic stability, i.e.

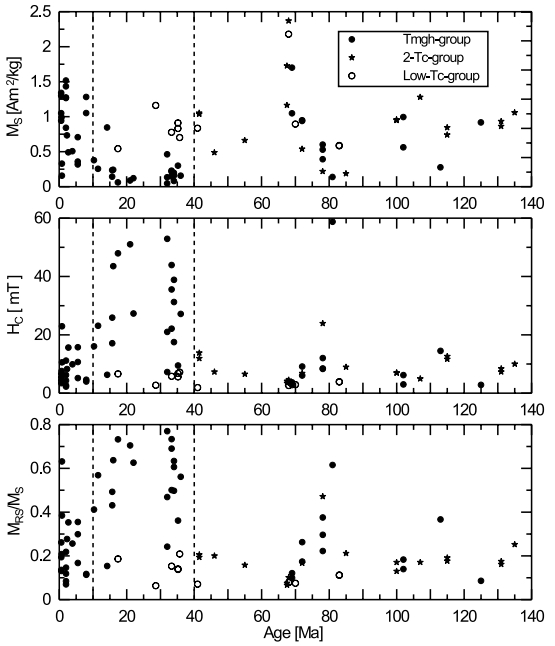

Fig. 4. Magnetic hysteresis properties plotted against age of the samples. Shown are saturation magnetization M_S, coercive force H_C, and the ratio of saturation remanence to saturation magnetization M_{RS}/M_S from VFTB measurements.

high H_C and M_{RS}/M_S values, in the same age range. There is no significant difference between the samples of the 2-T_C-group and Tmgh-group older than 40 Ma (although the data within each group are scattered).

Samples of the Low-T_C-group clearly have a higher saturation magnetization and a lower magnetic stability than the 10–40 Ma old Tmgh-group samples (Fig. 4). Their hysteresis parameters are similar to those found for the 0–10 Ma old samples of the Tmgh-group, with which they also share a low Curie temperature. It is therefore likely that, despite their ages higher than 15 Ma, the samples of the Low-T_C-group contain non-oxidized or only slightly oxidized titanomagnetites.

3.3. Influence of magnetic saturation on hysteresis parameters

As already mentioned above, due to the high magnetic stability of some samples, it was not possible to reach saturation during the hysteresis measurements with the VFTB. This imposes serious problems on the interpretation of the data, especially for the 10–40 Ma old samples of the Tmgh-group, which are of highest magnetic stability. Fig. 5a shows the upper (crosses) and lower (circles) branch of the hysteresis loop measured with the MPMS at room temperature between 0 and 5 T for sample 556-5-2(73), which has the highest magnetic stability (M_{RS}/M_S = 0.77 and H_C = 52.9 mT from measurements with the VFTB) of all samples of the Tmgh-group. The paramagnetic content was determined by a linear fit (full line) of both branches between 2 and 5 T and M_S determined by this method has exactly twice the value of M_{RS}. Hence, the magnetically most stable sample of the Tmgh-group yields $M_{RS}/M_S = 0.5$, which corresponds to the value theoretically expected for randomly oriented single-domain particles with uniaxial magnetic anisotropy [29]. The same hysteresis data are shown between 0 and 1.5 T in Fig. 5b. The upper and lower branch coincide for fields higher than 0.3 T, indicating that irreversible magnetization changes are restricted to fields lower than 0.3 T. For 0.3 T $< H <$ 1.5 T the ferrimagnetic (i.e. the titanomaghemite's) magnetization component approaches saturation reversibly with H by rotation of magnetization. The hysteresis loop of the same sample measured with the VFTB in fields up to 0.63 T is also shown in Fig. 5b. The estimate of the paramagnetic content between 0.5 and 0.63 T is affected by the (reversible) magnetization changes of the ferrimagnetic component, leading to an overestimate of the paramagnetic signal and a significant underestimate of M_S by this method (dashed line). As discussed above, irreversible magnetization changes are restricted to $H < 0.3$ T and consequently the M_{RS} measured by the VFTB is close to the value determined by the MPMS (the observed difference in M_{RS} and H_C for the two instruments is likely caused by different calibration of the two instruments). For the five samples measured with the MPMS the results are compared to the VFTB measurements. Except

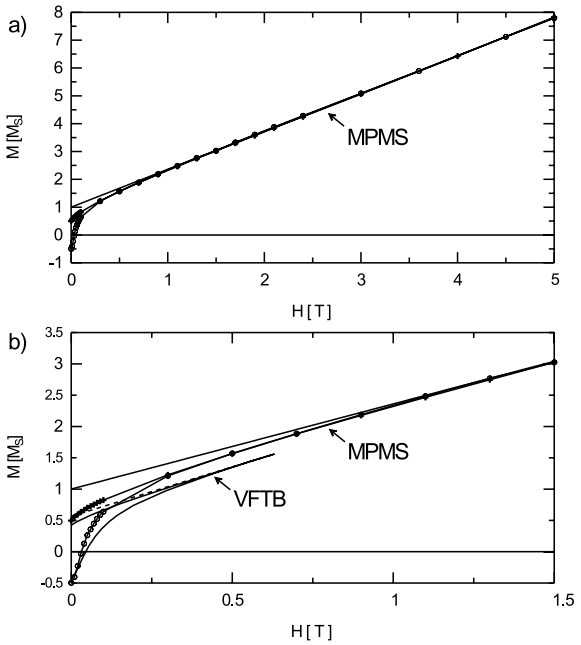

Fig. 5. Hysteresis loop at room temperature measured with the MPMS (a), crosses represent the upper and circles the lower branch of the hysteresis loop, and the VFTB (b) for sample 556-5-2(73). Additionally, the MPMS hysteresis loop is shown between 0 and 1.5 T in panel b. The paramagnetic content and M_S were determined by a linear fit of the data between 2 and 5 T for the MPMS (full line) and 0.5 and 0.63 T for the VFTB (dashed line). Magnetization is normalized on M_S determined from the MPMS measurement.

for sample 495-48-4(78), which gave considerable differences between VFTB and MPMS measurements (most likely due to a small scale inhomogeneity), a systematic trend with magnetic stability is found for the discrepancy in M_S between the two instruments (Table 1), whereas the discrepancy for M_{RS} is nearly constant. From this, we have to expect an overestimation of M_{RS}/M_S and an underestimation of M_S from VFTB measurements for magnetically stable samples. To account for this effect, the values of M_S measured by the VFTB were adjusted according to the results shown in Table 1, and under the assumption that samples with $M_{RS}/M_S < 0.4$ (measured with the VFTB) yield correct values for M_S. For this adjustment, later referred to as saturation correction, values for M_S were multiplied by a factor of 1.3 for $0.4 \leq M_{RS}/M_S < 0.57$, a factor of 1.75 for $0.57 \leq M_{RS}/M_S < 0.7$ and a factor of 1.85 for $0.7 \leq M_{RS}/M_S$.

3.4. Temperature dependence of the NRM of 10–40 Ma old ocean basalts

NRM intensities from room temperature to 600°C were measured with the Hotspin magnetometer for six of the 10–40 Ma old samples of the Tmgh-group, of which four are shown in Fig. 6 (dashed lines). Of each sample, two subsamples were measured separately, because only the NRM components perpendicular to the spinning axis are measured simultaneously by the instrument. The left plot (first subsample) shows the NRM intensity in the X–Z-plane and the right plot shows the NRM intensity in the Y–Z-plane (second subsample), where X, Y, and Z are arbitrarily chosen orthogonal sample coordinates. The similar temperature dependences of the NRM intensity for both planes of each sample (as well as a maximum deviation of 20° of the direction of magnetization within each plane, data not shown) suggest a simple single-component demagnetization behavior.

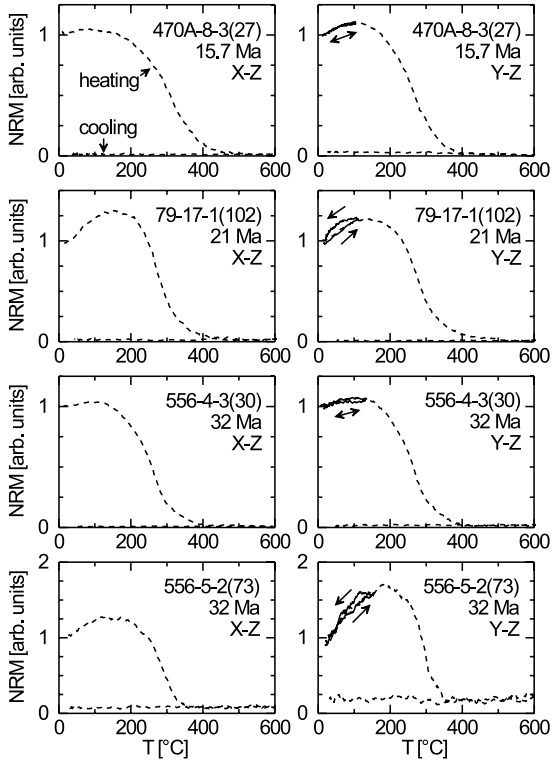

Fig. 6. Temperature dependence of the intensity of NRM. Dashed lines show heating/cooling cycles to 600°C, solid lines are minor heating/cooling cycles to the maximum of NRM.

All samples in Fig. 6 show an initial increase and a maximum of the NRM intensity between 100 and 200°C, before the NRM is unblocked at

Table 1
Comparison of VFTB and MPMS measurements

Sample	Age	M_{RS}/M_S	M_{RS}/M_S	M_{RS}	M_S
	[Ma]	VFTB	MPMS	VFTB result/MPMS result	
470A-8-3(27)	15.7	0.49	0.43	1.13	1.29
238-61-4(6)	34	0.63	0.44	1.22	1.77
572D-34-1(99)	16	0.64	0.45	1.22	1.72
556-5-2(73)	32	0.77	0.50	1.19	1.85
495-48-4(78)	22	(0.63)	(0.35)	(2.08)	(3.71)

≈400°C. The cooling curves are almost zero, indicating that no remanences are acquired in the instrument. The maximum in NRM intensity can be observed in both the X–Z- and Y–Z-planes, confirming that the total NRM intensity of the samples has a maximum above room temperature. After identifying the temperature at which the maximum in NRM intensity occurs from the measurement of the X–Z-plane and before heating the second subsample to 600°C, the second subsample was heated to the temperature of the maximum in NRM intensity and cooled to room temperature again. The NRM intensity during this process is reversible (full line with double-headed arrows in Fig. 6). A deviation to slightly higher NRM intensities at elevated temperatures during cooling was observed for two samples (full line with single-headed arrows in Fig. 6) and reflects a temperature hysteresis of the instrument. The reversibility rules out that the maximum in NRM intensity is due to thermal unblocking of an antiparallel NRM component and confirms that the NRM intensity follows the temperature dependence of the titanomaghemite's saturation magnetization.

The observed increase in NRM intensity due to Néel P-type or Néel N-type behavior for the samples shown in Fig. 6 ranges from ≈5% to ≈30%. Additionally, the 35.2 Ma old sample 77B-54-1(18) showed a reversible increase of 1% between room temperature and 110°C, and no increase was observable for 15.7 Ma old sample 470A-9-2(49) (data not shown).

4. Discussion

The 52 samples of the Tmgh-group represent the greatest proportion of the 93 samples studied. Judging from their Curie temperatures and reflected light microscopy, the Tmgh-group samples contain as the dominating phase titanomagnetites with $x \approx 0.6$ and titanomaghemites with increasing oxidation state with age. Their magnetic properties are strongly dependent on age and display a peculiar magnetic state in the age interval 10–40 Ma.

Only 23 of the total of 93 samples deviate from the above described typical magnetomineralogy of ocean basalts (the Low-T_C-group and samples with either magnetite or primary hemoilmenite). For the 2-T_C-group, consisting of 18 samples older than 40 Ma, magnetic properties are similar to those of the Tmgh-group in the same age interval. However, their magnetomineralogy could not be determined unequivocally. Therefore, we restrict the following discussion to results of Tmgh-group samples.

Typical for the 10–40 Ma old samples of the Tmgh-group are Curie temperatures between 280 and 360°C and a maximum in $M_S(T)$ above room temperature. The latter behavior is indicative for titanomaghemite with $x \geq 0.5$ and $z \geq 0.4$. This is known from studies on basalts [30,31] and confirmed by studies on synthetic samples [32,33]. This also confirms that the magnetominerals of the 10–40 Ma old ocean basalts are oxidized titanomagnetites with $x \approx 0.6$ and rules out the presence of titanomagnetites or titanomaghemites with $x < 0.5$, which might fortuitously have similar Curie temperatures [22]. Then, the observed range of $280°C \leq T_C \leq 360°C$ is indicative of an oxidation degree of approximately $0.65 \leq z \leq 0.85$ [9,11,22]. The lattice parameter determined for three samples in this age interval indicates $z \approx 0.9$ and $0.51 \leq x \leq 0.57$, which is lower than the expected value of $x = 0.6$.

The observed shape of $M_S(T)$, according to the classification of Néel [25], starts off for the very young samples with non-oxidized titanomagnetite with P-type behavior with the maximum in $M_S(T)$ below room temperature to P- or N-type behavior with a maximum in $M_S(T)$ above room temperature for oxidized titanomaghemite in the age range 10–40 Ma.

It is interesting to note that the Néel N-type of 22 Ma old sample 495-48-4(78) with $x = 0.57$ and $z = 0.81$ fits well to the development of the Néel type with maghemitization as observed by Readman and O'Reilly [22] for titanomaghemite with $x = 0.7$. They expected the occurrence of Néel N-type for a narrow oxidation range in the interval $0.73 < z < 0.86$.

For the samples older than 40 Ma, a further change in the shape of $M_S(T)$ to Néel P-type behavior with a maximum in M_S below room temperature is observed. This second change is evi-

dence for a further change in titanomaghemite composition, not accompanied by a significant increase of Curie temperature (ranging from 250 to 360°C) and oxidation state. We therefore speculate that this change in composition might reflect a redistribution of Fe cations between tetrahedral and octahedral sites in the titanomaghemite, rather than a further increase in oxidation state. Such a redistribution process would lead to a change in the shape of $M_S(T)$ (and the value of M_S at room temperature) but would not significantly affect T_C [34].

A further peculiarity of the Tmgh-group samples in the 10–40 Ma interval is a maximum in magnetic stability. The highest value of $M_{RS}/M_S = 0.5$ measured for sample 556-5-2(73) with the MPMS is unlikely to happen by accident, but suggests that these samples are single-domain with uniaxial anisotropy. This finding is in contrast to other studies on ocean basalts, implying that for those studies the titanomaghemites were not magnetically saturated or that our selection of samples does not include ocean basalts close to the pillow rim, where in general highest M_{RS}/M_S values are observed [35,36]. We interpret the observed increase in magnetic stability as a transformation of multi-domain or pseudo-single-domain particles in young ocean basalts to single-domain particles in 10–40 Ma old ocean basalt. This behavior does not necessarily need a corresponding change in the titanomaghemite grain size, but can be explained by a systematic change in magnetic material constants (particularly in M_S) due to maghemitization.

Our data fit very well to the domain-state model for titanomaghemites by Moskowitz [37]. His model predicts a pseudo-single-domain state for non-oxidized TM60 in the grain size range 0.5–40 μm, and a transformation to single-domain state of 2.5 μm grains for $z \geq 0.7$ and of 10 μm grains for $z \geq 0.8$. A more detailed study on the magnetic state causing this high magnetic stability is presented elsewhere [38], where it is argued that the high magnetic stability of these samples is caused by high internal stress in the order of 200 MPa in single-domain titanomaghemite grains.

The Tmgh-group suggests an age interval between 10 and 40 Ma where samples display the peculiar behavior discussed above. Taking into account the gradual nature of the oxidation process (e.g. [11]), these age limits can only be a rough estimate. Additionally, there is a lack of Tmgh-group samples between 36 and 69 Ma. Bleil and Petersen [9] calculated a geometric mean value for NRM intensity in the age interval from 10 to 30 Ma to demonstrate the low NRM values for about 20 Ma old ocean basalts. In order to compare our results, we calculated mean values of M_S for 10–30 Ma old samples. In Table 2, the geometric mean values for the saturation magnetization at room temperature of the ocean basalts after applying the saturation correction (as described in Section 3.3) are given for the age inter-

Table 2
Geometric mean values of saturation magnetization M_S for ocean basalts (bulk rock), inferred M_S for titanomagnetite/titanomaghemite minerals (mineral), and NRM intensity after [9] for different age intervals

Parameter	Based on	Age interval		
		0–5 Ma	10–30 Ma	69–125 Ma
M_S [A m^2/kg]	bulk rock	0.82 (0.43–1.55)	0.20 (0.09–0.43)	0.63 (0.32–1.25)
M_S [A m^2/kg]	bulk rock		0.18[a] (0.09–0.36)[a]	
M_S [%]	zero age value	100	24	77
M_S [kA/m]	mineral	125[b]	30[c]	96[c]
NRM[d] [%]	zero age value	100	≈28	≈70

All M_S values are from Tmgh-group samples after saturation correction (see text), range corresponding to standard deviation is given in parentheses.
[a] Age interval 10–40 Ma.
[b] For TM60 [28].
[c] Estimated.
[d] After Bleil and Petersen [9].

vals 0–5 Ma, 10–30 Ma and 69–125 Ma both in absolute values and as fraction normalized to the value for 0–5 Ma in percent. The mean values for M_S in the age intervals 10–30 and 10–40 Ma are very similar (Table 2). In the age interval 10–30 Ma, the saturation magnetization is four times lower than for the youngest samples (0–5 Ma) and approximately three times lower than for the older samples (69–125 Ma), which is in good agreement to a previous study [10]. In principle, both a systematic change of the saturation magnetization of the magnetominerals, as well as a systematic change in their content could explain that behavior. The latter explanation seems unlikely, as it would imply the simultaneous occurrence of a low titanomagnetite content for ocean basalts generated from the independent magma reservoirs of the Pacific and Atlantic oceans' ridges in the age interval 10–40 Ma. Furthermore, the decrease in saturation or spontaneous magnetization with maghemitization is known from synthetic samples [22,33] and natural titanomaghemites [39] and is intrinsically linked to the change of the Néel type. The underlying mechanism is thought to be low-temperature oxidation by migration of Fe ions out of the octahedral sites in the titanomaghemite's spinel structure. As the octahedrally coordinated Fe ions constitute the magnetically stronger ferrimagnetic sublattice, the titanomaghemite's net magnetization decreases (e.g. [9]) and eventually changes sign, as observed for two samples at $T < -180$°C (Fig. 3). Again, one could speculate that the higher value of M_S for the samples older than 40 Ma is connected to the observed change in the $M_S(T)$ curves. A possible explanation for this could be the increase of the net magnetization by the formation of vacancies on the tetrahedral sites either by further oxidation [9] or, as discussed above, the redistribution of Fe ions towards octahedral sites.

From the observed mean values of M_S and under the reasonable assumption of constant titanomagnetite/titanomaghemite content in the three age intervals, the mineral saturation magnetization of the titanomagnetites/titanomaghemites can be estimated. This is done in Table 2 by taking the saturation magnetization for TM60 (from [28], in units of magnetic moment per volume) as a starting value for the age interval 0–5 Ma. The value of ≈ 30 kA/m obtained for highly oxidized titanomaghemite in the age interval 10–30 Ma is in reasonable agreement with other studies [33,39].

The minimum in saturation magnetization for 10–40 Ma old ocean basalts coincides in age with the minimum in NRM intensities (from [9]; see Table 2), which suggests that both phenomena share the same cause. This view is supported by the high coercive force and high ratios of M_{RS}/M_S of the 10–40 Ma old samples, which coincide with a high magnetic stability of the NRM observed during alternating field demagnetization of ocean basalts with titanomaghemite of similar degree of oxidation [40].

However, it has to be kept in mind that the NRM of rocks is often carried by only a small proportion of its magnetominerals (e.g. [16]) and the hysteresis parameters of a rock sample might be misleading when interpreted as being typical for the magnetominerals carrying the NRM. Therefore we also measured the temperature dependence of the NRM intensity (Fig. 6) and found the same behavior for unblocking temperatures and Néel P-type or Néel N-type as in the strong-field magnetic measurements (T_C and $M_S(T)$) for samples of the age interval 10–40 Ma. This directly shows that maghemitiziation affects the NRM of ocean basalts in a similar way as it affects the bulk rock magnetic parameters, and links the decrease in NRM intensity within the first 10–40 Ma to the decrease of the spontaneous magnetization due to titanomagnetite maghemitization. Although the decrease of NRM intensity with titanomagnetite oxidation is well known for ocean basalts (e.g. [11] and references therein), the measurement of the NRM intensity at elevated temperature provides new experimental evidence for the influence of maghemitization on NRM by exploiting the occurrence of Néel P- and N-type behavior for the titanomaghemites. Table 2 shows that the relative change of the NRM intensity in percent is very similar to that of M_S at room temperature, with both parameters having $\approx 25\%$ of their starting value for approximately 10–30 Ma old ocean ba-

salts and ≈75% of the starting value for 69–125 Ma old ocean basalts.

This suggests that the age dependence of the mean NRM intensity of ocean basalts as described by Bleil and Petersen [9] is a product of the change of M_S with maghemitization. It appears therefore that long-term variations of the intensity of the Earth's magnetic field, which in principle could cause the age dependence of NRM intensity (but not the age dependence of M_S), are not necessary to explain the observed NRM behavior. Although paleointensity determinations on submarine basaltic glasses yield particularly low field intensities in the age interval 10–40 Ma [17,41], this is not supported by data from other lithologies from the database BOROKPINT.MDB [42], which yield a mean virtual dipole moment of $\approx 6.4\times10^{22}$ A m^2 for the age interval from 10 to 40 Ma from Thellier-type experiments of non-transitional samples, close to the present-day value of 8×10^{22} A m^2.

It can be concluded, therefore, that the majority of ocean basalts change their magnetic properties with age, in a manner that can be explained by titanomagnetite maghemitization. For 10–40 Ma old oceanic crust, this process leads to a low but very stable magnetization of the ocean basalts as well as Néel P- and N-type behavior, both for the saturation magnetization and for the NRM. The NRM and the saturation magnetization vary in approximately the same fashion during maghemitization.

Acknowledgements

We thank Özden Özdemir, Weiming Zhou and an anonymous reviewer for helpful comments. We would like to thank the Ocean Drilling Program (ODP) for providing the ocean basalt samples. Some of the measurements were conducted at the Institute for Rock Magnetism (IRM). The IRM is funded by the Keck Foundation, the National Science Foundation, and the University of Minnesota. J.M. and D.K. acknowledge a visiting fellowship from the IRM. This research was funded by the Deutsche Forschungsgemeinschaft.*[RV]*

References

[1] M. Prévot, G. Remond, R. Caye, Étude de la transformation d'une titanomagnétite en titanomaghémite dans une roche volcanique, Bull. Soc. Fr. Minéral. 91 (1968) 65–74.
[2] E. Irving, The Mid-Atlantic-Ridge at 45° N. XIV. Oxidation and magnetic properties of basalts; review and discussion, Can. J. Earth Sci. 7 (1970) 1528–1538.
[3] H.P. Johnson, J.M. Hall, A detailed rock magnetic and opaque mineralogy study of the basalts from the Nazca Plate, Geophys. J. R. Astr. Soc. 52 (1978) 45–64.
[4] N. Petersen, P. Eisenach, U. Bleil, Low temperature alteration of the magnetic minerals in ocean floor basalts, in: M. Talwani (Ed.), Deep Drilling Results in the Atlantic Ocean: Ocean Crust, Maurice Ewing Series 2, American Geophysical Union, Washington, DC, 1979, pp. 169–209.
[5] W. O'Reilly, S.K. Banerjee, The mechanism of oxidation in titanomagnetites and self-reversal, Nature 221 (1966) 26–28.
[6] W. Zhou, D.R. Peacor, R. Van der Voo, Single-domain and superparamagnetic titanomagnetite with variable Ti content in young ocean-floor basalts: No evidence for rapid alteration, Earth Planet. Sci. Lett. 150 (1997) 353–362.
[7] J.M. Hall, Does TRM occur in oceanic Layer 2 basalts?, J. Geomagn. Geoelectr. 29 (1977) 411–419.
[8] F.J. Vine, D.H. Matthews, Magnetic anomalies over ocean ridges, Nature 199 (1963) 947–949.
[9] U. Bleil, N. Petersen, Variations in magnetization intensity and low-temperature titanomagnetic oxidation of ocean floor basalts, Nature 301 (1983) 384–388.
[10] H.P. Johnson, J.E. Pariso, Variations in oceanic crustal magnetization: Systematic changes in the last 160 million years, J. Geophys. Res. 98 (1993) 435–445.
[11] W. Zhou, R. Van der Voo, D.R. Peacor, D. Wang, Y. Zhang, Low-temperature oxidation in titanomagnetite to titanomaghemite: A gradual process with implications for marine magnetic anomaly amplitudes, J. Geophys. Res. 106 (2001) 6409–6421.
[12] N.A. Wittpenn, C.G.A. Harrison, W. Handschuhmacher, Crustal magnetization in the South Atlantic from inversion of magnetic anomalies, J. Geophys. Res. 94 (1989) 15463–15480.
[13] E. Geiss, N. Petersen, U. Bleil, Amplitude variation of marine magnetic anomalies, Geol. Rundsch. 78 (1989) 741–752.
[14] K. Sayanagi, K. Tamaki, Long term variations in magnetization intensity with crustal age in the Northeast Pacific, Atlantic and Southeast Indian Ocean, J. Geophys. Res. 12 (1992) 2369–2372.
[15] C. Raymond, J.L. LaBrecque, Magnetization of the oceanic crust: Thermoremanent magnetization or chemical remanent magnetization, J. Geophys. Res. 92 (1987) 8077–8088.
[16] D.V. Kent, J. Gee, Grain size-dependent alteration and the magnetization of oceanic basalts, Science 265 (1994) 1561–1563.

[17] M.T. Juárez, L. Tauxe, J. Gee, T. Pick, The intensity of the Earth's magnetic field of the past 160 million years, Nature 394 (1998) 878–881.
[18] P.J.C. Ryall, J.M. Ade-Hall, Radial variation of magnetic properties in submarine pillow basalt, Can. J. Earth Sci. 12 (1975) 1959–1969.
[19] M.R. Perfit, W.W. Chadwick, Jr., Magmatism at mid-ocean ridges: Constraints from volcanological and geochemical investigations, in: W.R. Buck, P.T. Dalaney, J.A. Karson, Y. Lagabrielle (Eds.), Faulting and Magmatism at Mid-Ocean Ridges, Geophysical Monograph 106, Am. Geophys. Union, Washington, DC, 1988, pp. 59–115.
[20] C.S. Grommé, T.L. Wright, D.L. Peck, Magnetic properties and oxidation of iron-titanium oxide minerals in Alae and Makaopuhi Lava Lakes, Hawaii, J. Geophys. Res. 74 (1969) 5277–5293.
[21] J. Matzka, Besondere magnetische Eigenschaften der Ozeanbasalte im Altersbereich 10 bis 40 Ma, Ph.D. Thesis, Ludwig-Maximilians-Universität München, 2001.
[22] P.W. Readman, W. O'Reilly, Magnetic properties of oxidized (cation-deficient) titanomagnetites (Fe, Ti, $\square)_3O_4$, J. Geomagn. Geoelectr. 24 (1972) 69–90.
[23] P. Ramdohr, Die Erzmineralien und ihre Verwachsungen, Akademie-Verlag, Berlin, 1955.
[24] Ö. Özdemir, Inversion of titanomaghemites, Phys. Earth Planet. Inter. 46 (1987) 184–196.
[25] M.L. Néel, Propriétés magnétiques des ferrites; ferrimagnéetisme et antiferromagnétisme, Ann. Phys. 12 (1948) 137–198.
[26] A.F. Buddington, D.H. Lindsley, Iron-titanium oxide minerals and synthetic equivalents, J. Petrol. 5 (1964) 310–357.
[27] R.B. Hargraves, N. Petersen, Notes on the correlation between petrology and magnetic properties of basaltic rocks, Z. Geophys. 37 (1971) 367–382.
[28] D.J. Dunlop, Ö. Özdemir, Rock Magnetism: Fundamentals and Frontiers, Cambridge Studies in Magnetism, Cambridge University Press, Cambridge, 1997, 573 pp.
[29] E.C. Stoner, E.P. Wohlfarth, A mechanism of magnetic hysteresis in heterogeneous alloys, Philos. Trans. R. Soc. Ser. A 240 (1948) 599–642.
[30] A. Schult, Self-reversal of magnetization and chemical composition of titanomagnetites in basalts, Earth Planet. Sci. Lett. 4 (1968) 57–63.
[31] A. Schult, On the strength of exchange interactions in titanomagnetites and its relation to self-reversal of magnetization, Z. Geophys. 37 (1971) 357–365.
[32] Ö. Özdemir, W. O'Reilly, High-temperature hysteresis and other magnetic properties of monodomain titanomagnetites, Phys. Earth. Planet. Inter. 25 (1981) 406–418.
[33] Ö. Özdemir, W. O'Reilly, Magnetic hysteresis properties of synthetic monodomain titanomaghemites, Earth Planet. Sci. Lett. 57 (1982) 437–447.
[34] W. O'Reilly, The identification of titanomaghemites: model mechanisms for the maghemitization and inversion processes and their magnetic consequences, Phys. Earth Planet. Inter. 31 (1983) 65–76.
[35] J. Gee, D.V. Kent, Magnetic hysteresis in young mid-ocean ridge basalts: Dominant cubic anisotropy?, Geophys. Res. Lett. 22 (1995) 551–554.
[36] J. Gee, D.V. Kent, Calibration of magnetic granulometric trends in oceanic basalts, Earth Planet. Sci. Lett. 170 (1999) 377–390.
[37] B.M. Moskowitz, Theoretical grain size limits for single-domain, pseudo-single-domain and multi-domain behavior in titanomagnetite ($x = 0.6$) as a function of low-temperature oxidation, Earth Planet. Sci. Lett. 47 (1980) 285–293.
[38] J.P. Hodych, J. Matzka, Estimating saturation magnetostriction for single-domain titanomaghemite in oceanic basalts: an indirect method using the effect of axial compression on saturation remanence, submitted to Geophys. J. Int.
[39] B.M. Smith, Consequences of the maghemitzation on the magnetic properties of submarine basalts: synthesis of previous works and results concerning basement rocks from mainly D.S.D.P. legs 51 and 52, Phys. Earth Planet. Inter. 46 (1987) 206–226.
[40] N. Petersen, U. Körner, Magneto-mineralogy and magnetic properties of ocean floor basalts, in: K. Subbarao (Ed.), Magnetism - Rocks to Superconductors, Geological Society of India Memoir 29, Geol. Soc. India, Bangalore, 1994, pp. 1–25.
[41] P.A. Selkin, L. Tauxe, Long-term variations in palaeointensity, Phil. Trans. R. Soc. Lond. 358 (2000) 1065–1088.
[42] V.P. Shcherbakov, G.M. Solodovnikov, N. Sycheva, Variations in the geomagnetic dipole during the past 400 million years (volcanic rocks), Izv. Phys. Solid Earth 38 (2002) 113–119.